Baltic Astronomy, vol. 8, 73–96, 1999.

GAIA SPECTROSCOPY: PROPOSING THE 8500–8750 Å REGION AND EVALUATING THE PERFORMANCES

Ulisse Munari

Padova and Asiago Astronomical Observatories, Italy
CISAS, University of Padova, Italy
(e-mail: munari@pd.astro.it)

Received February 10, 1999.

Abstract. We propose the *Gaia* spectroscopic observations to be performed over the wavelength interval 8500–8750 Å, with an optimal dispersion of 0.25 Å/pix (or 1000 pixels budget per spectrum) and a 2 pixel PSF. In this paper, on the base of extensive observations as well as synthetic spectra and simulations, we review the spectroscopic performances expected for *Gaia*: radial and rotational velocities, spectral classification, detection of mass-loss and spectral peculiarities, chemical abundance analysis and reddening estimates from the 8620 Å diffuse interstellar band. Lower dispersion spectra (corresponding to smaller pixel budgets) are considered too.

Key words: stars: infrared spectra, synthetic spectra, spectral classification, abundances – ISM: extinction, interstellar bands – orbiting observatories: Gaia

1. INTRODUCTION

The astrometric and photometric mission *Gaia* by ESA is currently planned to host a spectrometer to measure radial velocities and therefore to provide the 6th component of the phase–space coordinates for all stars brighter than a given limit (e.g. $I \approx 14$ mag, the exact limit will be set by the final optical design, spacecraft scanning law, global throughput and S/N threshold to trigger the detection during crossing of the focal plane and dimensions of the

latter). The foreseen operational constraints for the *Gaia* spectrometer are rather severe: an observable interval $\Delta\lambda \leq 300$ Å, a 300 to 1000 pixel budget per spectrum, a constant exposure time (set by the spacecraft scanning law and focal plane dimensions) and about 150 spectra per target over the mission lifetime. This means – by trivial statistics – that for the majority of targets *epoch-spectra* will be obtained at fairly low S/N (about 6–10) but *mission-spectra* will score high S/N ($\geq$100). High resolution, high S/N mission-spectra will open the possibility to investigate many physical parameters other than just the radial velocities, as sketched in Table 1. Fixing the basic requirements for *Gaia* spectroscopy means to investigate the response to all the entries in Table 1, with radial velocities playing the leading role.

The *Gaia* spectroscopic databank at the end of the mission will include so vast amount of stars and information that it will affect future research to an extent similar or even greater than the Henry Draper (HD) survey affected 20th century astrophysics. The *Gaia* spectroscopic databank will be the reference for several decades. Therefore, it is of great relevance that the wavelength range, where *Gaia* will perform its observations, is easily accessible from the ground, with the lowest possible contamination by telluric absorptions (cf. Fig. 1).

2. STRATEGY

Gaia will record for each target star ~150 epoch-spectra over the mission life-time. By adding them up a mission-spectrum will be obtained. A realistic example of both epoch- and mission-spectra is given in Fig. 2. They directly set the following strategy:

(1) for non-time-dependent quantities, like spectral classification, chemical composition, reddening and rotational velocity it will be possible to rely for all *Gaia* targets on the high S/N mission-spectrum. It will be therefore possible to use and to study even fairly weak spectral features (equivalent widths $EW \geq 0.02$ Å);

(2) time-dependent quantities like radial velocities in binaries and pulsating stars, spectral peculiarities (e.g. emission lines) and signatures of mass-loss (e.g. P Cyg profiles) have to be derived from individual epoch-spectra. It is therefore relevant to this aim that the *Gaia* spectral region will include sensitive features which are strong enough to be detectable on weak epoch-spectra;

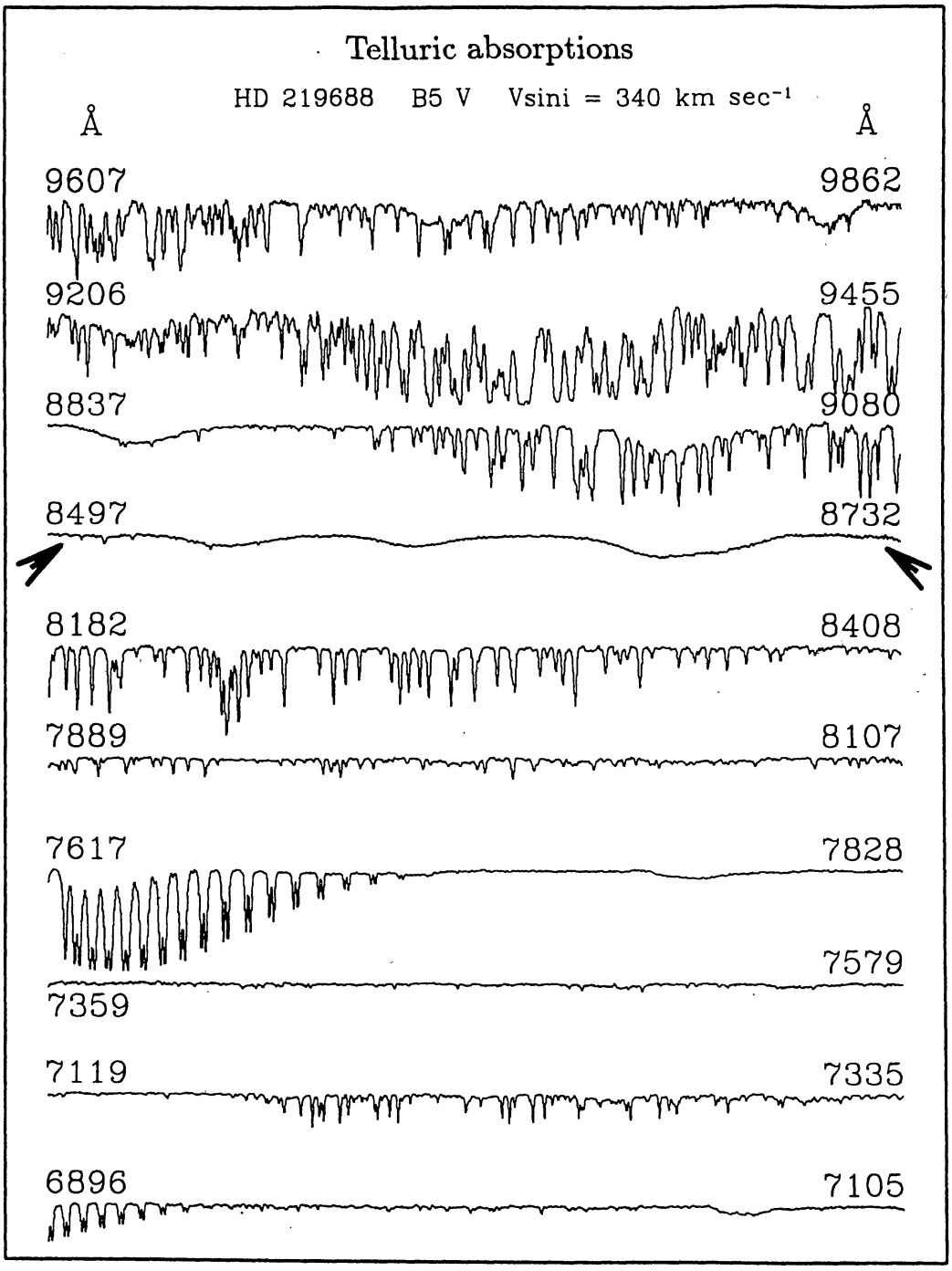

Fig. 1. Telluric absorptions in the red/near-infrared region from an Echelle spectrum of the fast rotating B5 V star HD 219688. The 8500–8750 Å interval, proposed for *Gaia* (indicated by the arrows), is clearly less affected by Earth's atmosphere. The stellar absorption lines are very broad and shallow, while all sharp lines are of telluric origin.

Table 1. Expected outcomes of *Gaia* spectroscopy.

• Radial velocities	• Spectral classification
– Galactic kinematics	• Chemical abundances
– Orbits of binaries	• Rotational velocity
– Stellar pulsations	• Mass-loss
– Internal kinematics of aggregates	• Peculiarities
– Extra-solar planet detection	• Signatures of reddening

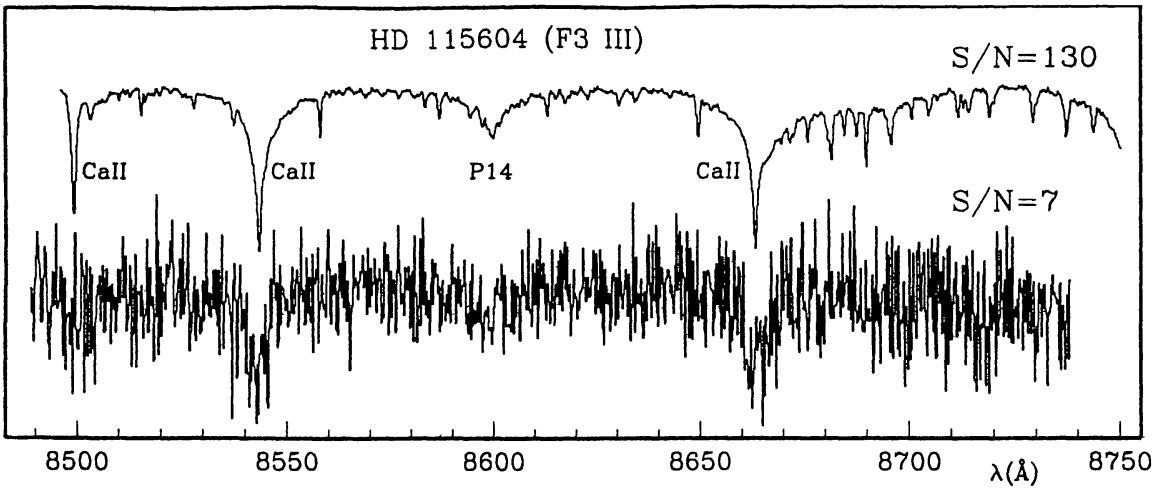

Fig. 2. Low and high *S/N* spectra of the F3 III star HD 115604 as examples of the epoch- and mission-spectra of a faint *Gaia* target.

(3) *Gaia* is going to observe spectroscopically a huge and unbiased number of stars (several 10^6), of the widest range in metallicity, temperature, gravity, galactic population, etc. The same stars will rank among those scoring the most accurate astrometry and photometry provided by *Gaia* itself. Therefore any relation between the physical quantities will be naturally self-calibrated in-situ by *Gaia*, from scratch and in an unbiased way without any specific necessity to rely on ground-based calibrations.

3. PROPOSING THE 8500–8750 Å INTERVAL

It is desirable that the most accurate spectroscopic results will be secured by *Gaia* on the same stars for which it will obtain the best astrometric results (distance and tangential motion). Current population models of the Galaxy show that the stars with best *Gaia* astrometric results will be F, G and K stars. Their energy distributions, already intrinsically peaked toward the red, are made even redder by interstellar extinction that is expected to affect a significant fraction of the targets (especially all those laying in the Milky Way). To maximize the photon harvest the *Gaia* spectrometer will have therefore to work in the red/near-infrared (hereafter, near-IR) spectral range. It is worth to note that the Doppler shift in the red/near-IR is twice larger compared to the classical blue region of ground-based observations.

What in the red/near-IR region with $\Delta\lambda \approx 300$ Å interval is best suited for *Gaia* spectroscopy? In F, G, K and M stars the strongest spectral signatures longward of Hα are the K I doublet around 7680 Å, the Na I doublet at 8194 Å and the Ca II triplet around 8600 Å. Their basic properties can be summarized as follows.

3.1. K I 7664.907, 7698.979 Å resonant doublet

These lines show moderate equivalent widths ($EW = 0.1$–0.4 Å) and a complicated luminosity effect (strong in class V and I, weak in class III). Additional problems with the K I lines are:

(*a*) The K I doublet is a strong interstellar absorption feature ($EW = 0.25$ Å for $E_{B-V} = 1.0$) and, unless the background star has a high radial velocity, interstellar and stellar components irremediably blend together;

(*b*) The K I lines fall at the core of a strong TiO band (head at 7590 Å), which significantly complicates the usage of the doublet in late-K, M and S stars (where the pseudo-continuum inside the band may go down to ~10 % of the continuum outside the band, and on this depressed continuum the K I lines have to exhibit their absorption profiles);

(*c*) The K I doublet falls on the wing of the strongest telluric absorption band (atmospheric A-band by O_2, cf. Fig. 1). The contamination is quite severe: one of the two K I lines (at 7664.907 Å) is in λ-coincidence with a component of the telluric A-band. The

telluric line is stronger than K I 7664.907 Å even in M2 Ia stars (where the K I doublet reaches its peak intensity). Therefore, profitable observations of the K I doublet and the surrounding region from the ground are quite difficult;

(*d*) O, B and A-type stars do not show significant absorption lines in this region, except of the O I blend at 7774 Å. This blend appears at B3 and disappears at F8, passing through a maximum EW = 0.7 Å at A3 V and EW = 2.0 Å at A6 I. The O I blend is a weak luminosity indicator for classes V–IV–III–II, with only class I clearly distinguished from the others;

(*e*) In F, G, K and M stars the 300 Å region around the K I doublet lacks other strong absorption lines, which is a severe problem for radial velocities and chemical abundance analysis.

3.2. Na I 8193.256, 8194.821 Å non-resonant doublet

It is stronger than the above K I doublet: the EW is 2.2 Å at M1 V, 0.6 Å at M1 III and 0.1 Å at M1 I. The luminosity effect is quite complicated: it is negative in M-stars, null in G-stars (EW = 0.7 Å at G5 III) and becomes positive in F-stars (EW = 0.6 Å at F8 III). In giants EW remains at 0.6 Å over the whole sequence of F, G, K and M stars and, therefore, the Na I doublet is not very useful in the spectral classification of evolved stars. Being non-resonant, Na I doublet has no problems with contamination by interstellar components which are severe for K I. However, there are other problems with the Na I doublet:

(*a*) The Na I lines are spaced only by 1.6 Å and a resolution better than 0.5 Å (dispersion $\leq$0.25 Å/pixel) is necessary to resolve accurately the doublet;

(*b*) There is a complicated structure of the super-imposing TiO band heads around the Na I doublet. They could interfere with automatic radial velocity measurements of the epoch-spectra (particularly for mismatches between the target and template spectral types);

(*c*) O, B and A-type stars do not show significant absorption lines in the region around the Na I doublet. Only a few N I lines are of interest there, in particular the 8216.28 Å line that becomes visible at A0, peaks around A4 and disappears at F4. N I 8216.28 Å is not generally seen in dwarfs, while in supergiants it may reach EW = 0.4 Å. Unfortunately, N I 8216.28 Å falls right at

the core of the telluric z-band and therefore its ground-based observation is always very problematic (at best);

(*d*) No doubt, for the Na I doublet the most disturbing problem is the extremely severe telluric H_2O z-band (cf. Fig. 1), with a forest of strong lines (several tens of them may absorb 40 % or more of underlying continuum). Being produced by water vapor, the z-band is also weather-dependent and time-variable. If the pre-launch and post-mission ground-based observations are a relevant issue, this region looks like a rather poor choice.

3.3. Ca II 8498.018, 8542.089, 8662.140 Å non-resonant triplet

These lines are by far the strongest in the red/near-IR reaching $EW = 6$ Å in G–K supergiants. Even in dwarfs the Ca II lines are remarkable with an $EW \geq 3$ Å from F8 V to M8 V. Ca II lines appear around B8 and dominate throughout M-stars, with a positive and strong luminosity effect. Being non-resonant, they have no problems with contamination by interstellar components. There are further advantages in selecting the region around near-IR Ca II triplet for *Gaia* operation (several other will become evident later on):

(*a*) this is the near-IR region, less affected by telluric absorptions (cf. Fig. 1), with very few, sparse and weak H_2O lines of $EW \leq 0.05$ Å (which disappear in spectra obtained in dry nights);

(*b*) there is no nearby molecular band head which can lower the accuracy of radial velocity measurements in automatic cross-correlation;

(*c*) the Ca II lines are always so intense in F, G, K and M stars that the cross-correlation can derive useful radial velocities even from severely under-exposed spectra (like $S/N = 7$ of Fig. 2);

(*d*) around Ca II there are hydrogen Paschen, He I, He II and strong N I absorption lines that can be profitably used to classify the spectra and to measure radial velocities of O, B and A stars;

(*e*) strong and numerous lines of iron-peak and α-elements (particularly Fe I, Ti I, Mg I, Si I) cluster around the Ca II triplet; these lines are remarkable in cool star spectra.

3.4. To be precise

The 250 Å wavelength interval which we have explored and propose for *Gaia*, is actually extended over 8493–8743 Å (the 8500–

8750 Å cited along the whole of this paper is just a rounding-off for reader's convenience). With the 250 Å interval so placed, (1) the bluest Ca II component (at 8498.018 Å) and Paschen 16 are close to the blue edge but inside the recorded region even for high velocity stars, and (2) the longward limit extends enough toward the red to include N I 8728.88, Si I 8742.600, Mg I 8736.000, Ti I 8734.700 and He I 8733.4 Å lines. Paschen 12 (8750.475 Å) falls at the border of the region we investigated.

4. INVESTIGATION OF THE PROPOSED WAVELENGTH INTERVAL

After selecting the spectral range from the above considerations, in December 1997 we embarked in an all-out campaign to investigate the response of the 8500–8750 Å interval to the *Gaia* demands. We have made massive use of telescopes, computations with the Kurucz synthetic spectra and simulations. The observations were carried out with the Echelle spectrometer mounted at the Cassegrain focus of the 1.82 m telescope operated by Osservatorio Astronomico di Padova on top of Mt. Ekar, Asiago (Italy). The detector was a THX31156 Thomson CCD 1024×1024 pixels, 19 μm each. Great care was placed in maintaining the dispersion and resolution, constant over the whole observing campaign (so far 48 scheduled nights in total). The observations have been completed in 12 months (Dec. 1997 – Dec. 1998), which greatly contributed to the homogeneity of the data. Reduction of the spectra has been performed in a standard way under IRAF. Observations will continue throughout 1999.

We adopted a 0.25 Å/pixel dispersion and a $\lambda/\Delta\lambda = 20\,000$ resolving power (which sets the resolution to 0.43 Å, equivalent to 1.75 pixels in the PSF-FWHM sense). The whole 250 Å spectrum is therefore recorded by over 1000 pixels. Observations at other dispersions with the Echelle and other spectrographs in Asiago have been performed, principally to investigate the effects on radial velocities. Some results will be given in the last section.

Preliminary results of our investigations of the 8500–8750 Å range have been reported in a series of documents to the ESA Photometric Working Group on *Gaia* (documents UM-PWG-003, -004, -005, -006). Full details will appear in a series of papers to appear in Astronomy & Astrophysics journal, some of which have already been submitted, while others are in preparation. The interested reader is

referred to them for the details not given here (including extensive literature references). The series includes the following papers.

Paper I (Munari & Tomasella, submitted) is an extensive mapping of the MK system (122 standards, covering types O4 to M8 and luminosity classes V through I). Fig. 4 is taken from it;

Paper II (Munari et al., to be submitted) concerns an extensive investigation of the correspondence between the reddening and the equivalent width of the diffuse interstellar band at 8620 Å. Figs. 9a and 9b are preliminary versions from this paper;

Paper III (Tomasella & Munari, in preparation) deals with the spectra of more than a hundred peculiar stars of all types. Figs. 6 and 7 are taken from this paper;

Paper IV (Castelli & Munari, in preparation) builds a library of more than 600 Kurucz spectra computed over the 8500–8750 Å region at the same 20 000 resolving power as the Asiago Echelle observations. Fig. 9 is taken from this paper.

Additional papers will deal with the accuracy of chemical abundance analysis, the precision of radial and rotation velocities, membership segregation by radial velocities, stellar pulsations traced by radial velocities, the accuracy of spectroscopic orbits and diagnostic line ratios (preliminary results have been already included in some UM-PWG documents and are briefly outlined in the next sections as well as in Figs. 2, 5 and 8 and Tables 2 and 3).

5. EVALUATING THE POSSIBILITIES

In the following subsections we review the *Gaia* spectroscopic performance on the basis of spectroscopic observations and simulations we have done to evaluate the response to Table 1 items.

5.1. Spectral classification

Classification of O and early-B stars is possible but not particularly straightforward due to weakness of Paschen, He I and He II lines. Starting with type B8, the Ca II triplet lines become visible and over the whole B8–M8 sequence the classification is made easy by a constantly growing number of other strong metallic lines (cf. Figs. 3 and 4). The relative intensity of Ca II and Paschen lines offers for B8 to F8 stars the same diagnostic tool as provided by the Balmer and Ca II H and K lines in the classical blue region. In G,

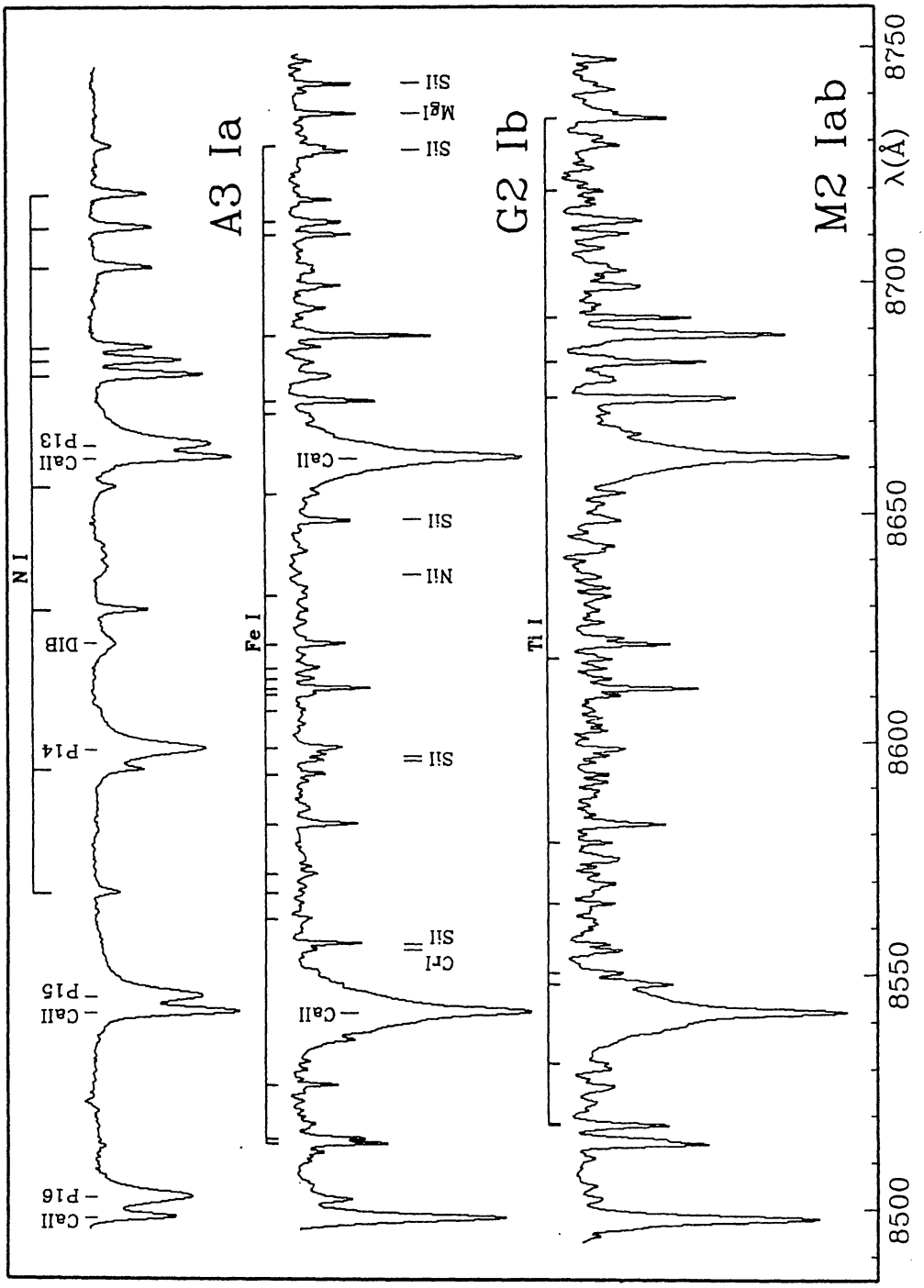

Fig. 3. Spectra of A, G and M supergiants with identification of some of the strongest lines. Sequences of N I, Fe I and Ti I absorptions characterize the A, G and M spectra, respectively. Ca II lines become visible at B8 and dominate throughout the M stars, while the Paschen lines disappear at ∼F8.

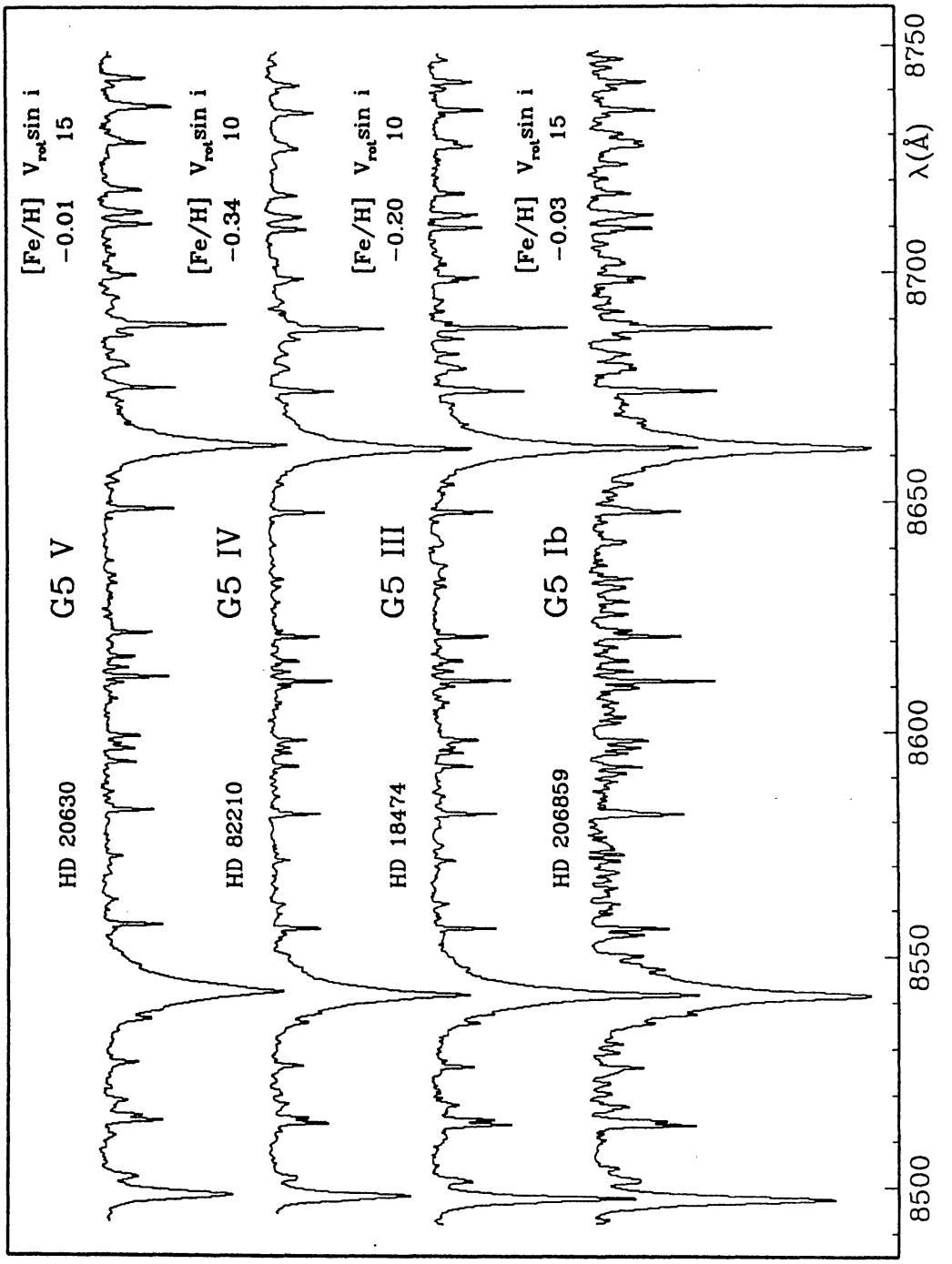

Fig. 4. Luminosity sequence at G5 (MK standards) as an example of the excellent classification potential of the 8500–8750 Å region. Metallicities and rotational velocities are given. These spectra nicely document the degeneracy between luminosity and metallicity on a cursory inspection. The effect is best illustrated by comparing stars of similar metallicity and different luminosity, e.g. HD 20630 (G5 V) with HD 206859 (G5 Ib), and HD 82210 (G5 IV) with HD 18474 (G5 III).

K and M stars Paschen lines are not more visible, the Ca II triplet progressively saturates and the classification shifts more and more to other metallic lines (particularly Si I, Mg I, Fe I and Ti I). Given the similar number of metallic lines per wavelength interval, the 8500–8750 Å region offers the same classification accuracy as the classical blue region (for example, taking the 250 Å interval 3870–4120 Å centered on the Ca II H and K lines and the H8, Hϵ and Hδ Balmer lines).

5.2. Continuous vs. discrete classification schemes

Over the 8500–8750 Å region several metallic ions show absorption lines of the same multiplet as well as from multiplets of largely different excitation potential (for example, the strongest Fe I lines come from multiplets Nos. 60, 449, 401, 623, 713, 1050, 1153, ..., 1272, ranging in excitation potential from 2.17 to 5.00 eV). This offers a bright prospect for *quantitative* classification and classification based on ratios of equivalent widths.

Real stars are continuously distributed in temperature, luminosity, metallicity, etc., but all past and present classification systems have forced them into discrete bins. With an expected harvest of several 10^6 stars observed under extremely homogeneous conditions, *Gaia* spectroscopy is perfectly suited to change the classification process from the present discrete step approach to a continuously varying scheme, based on quantitative line ratios and not restricted to the best match with a library of standards.

For all spectroscopic targets *Gaia* will provide precise (*a*) distances (or luminosities) from astrometry, (*b*) temperatures from broad- and narrow-band photometry, (*c*) metallicities from spectra. An *accurate* and *continuous* classification in terms of temperature, luminosity and metallicity (the missing 3rd parameter in the MK system) will be therefore defined by ratios of equivalent widths, and such a fully consistent system could be easily exported to future ground-based spectrometry.

5.3. Radial velocities

The main reason to have a spectrometer on *Gaia* is to measure radial velocities. Our preliminary results for the expected accuracies

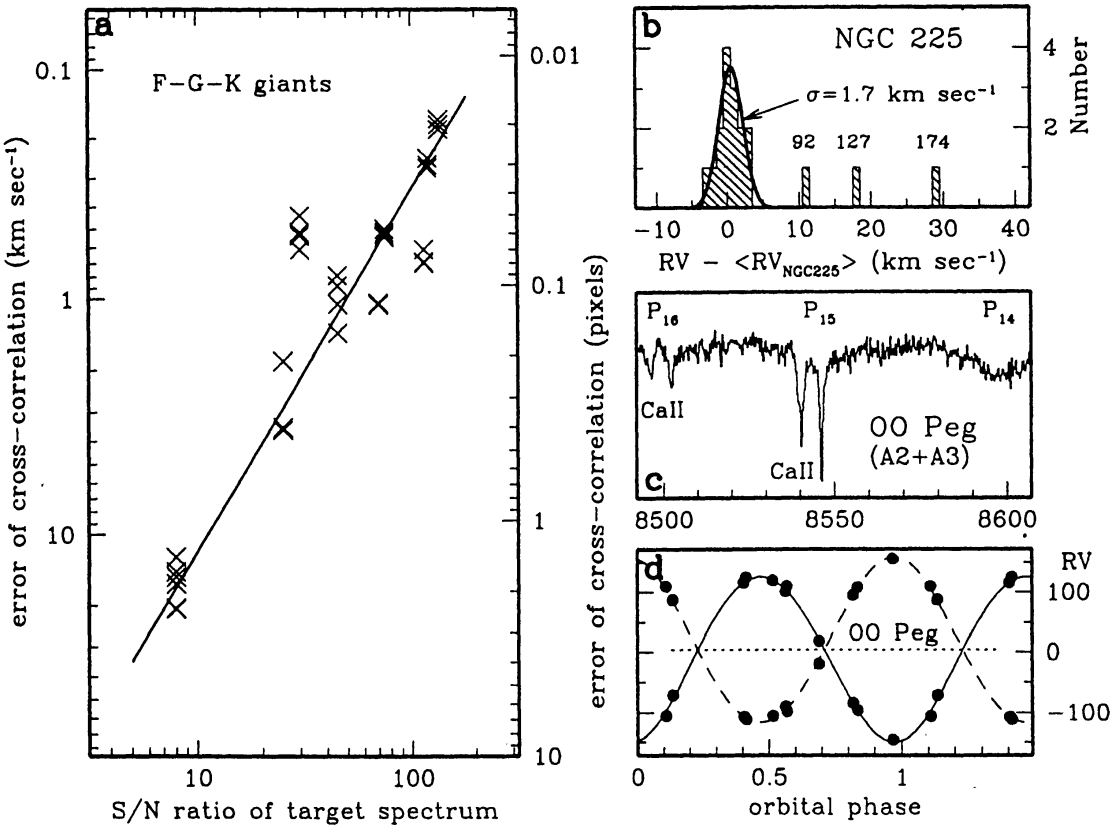

Fig. 5. (a): cross-correlation error as a function of S/N ratio of the target spectrum (template spectrum with $S/N \geq 300$; template and target spectra intentionally mis-matched in spectral type); (b): dispersion of radial velocities and discovery of spurious astrometric members for 18 stars in the young open cluster NGC 225; (c): zoomed-in spectrum of the double-lined eclipsing binary OO Peg (A2 V + A3 V); both components are easily separated in the Ca II lines but not in the Paschen lines; (d): spectroscopic orbit of the double-lined eclipsing binary OO Peg from the radial velocities of the Ca II lines.

from cross-correlation techniques are briefly summarized in Fig. 5 and Table 2.

The performance of the region on cool stars is indeed excellent. Radial velocities can be measured to better than 1 km/s on K–M epoch spectra with $S/N \geq 18$. The same accuracy is achievable on epoch spectra of G-stars with $S/N \geq 30$ and F-stars with $S/N \geq 45$.

This means that after averaging over ~150 epoch-spectra *Gaia* will be able to provide over the whole sky an extremely homogeneous network of thousands of radial velocity standards accurate to 0.01 km/s.

To the reader's benefit, Fig. 4 compares a $S/N = 7$ and $S/N = 130$ spectra of the same F3 III star, which might be considered respectively as examples of an epoch-spectrum and the mission-spectrum for a target at the faint end of *Gaia* sensitivity. The radial velocity on the $S/N = 7$ spectrum can still be extracted with an accuracy of 20 km/s (cf. Table 2).

The performance on hot stars is satisfactory for all but the weakest targets (cf. the B4 V entry in Table 2). O and B stars bright enough to produce $S/N \geq 35$ epoch-spectra will have their average radial velocity determined to a precision of ~ 2 km/s over the *Gaia* mission.

5.3.1. Spectroscopic binaries

The errors of radial velocities decrease towards cooler spectral types and, therefore, the accuracy of spectroscopic orbits increases towards later spectral types. However, even for early A-type binaries the accuracy that *Gaia* can reach is already remarkable as Fig. 5 shows for of the eclipsing binary OO Peg. OO Peg is a short period, A2+A3 double-lined binary of large amplitude (maximum separation is 316 km/s). The spectrum in Fig. 5c has been taken close to maximum separation, nevertheless Paschen lines do not split yet. Instead, the Ca II lines separate perfectly and allow accurate radial velocity measurements for both components of the binary. The standard deviation from the preliminary spectroscopic orbit of the eleven observations in Fig. 5d is just 1.1 km/s. At this level of precision, a few more observations will allow to measure masses of the A2 and A3 components accurate to better than 1 %. It is worth to remember that the best mass-luminosity and mass-radius relations (errors ≤ 1 %), presently available in literature, are based on less than 60 eclipsing binaries. This is a field were *Gaia* can impact dramatically, with stellar masses and radii measured to better than 1 % for thousands of eclipsing binaries.

Table 2. Errors in km/s of the radial velocities as a function of the S/N ratio of the program star spectrum. For example, ten spectra of HR 3454, each with $S/N = 40$, when cross-correlated against a $S/N = 350$ spectrum of HD 21483 (B3 III) show a dispersion of the resulting radial velocities of 23 km/s (or 2.60 pixels). The template star spectra here used all have $S/N \geq 300$. The spectra are of 1024 pixels length, 8493–8743 Å range, 0.25 Å/pix dispersion and 0.43 Å resolution.

		η Aur	HD 21483	HD 224055
		B3 V	B3 III	B3 Ia
HR 3454 (B4 V)	$S/N = 80$	19	15	6
	40	25	23	14
	8	158	115	59
		HR 458	HR 8905	HR 7796
		F8 V	F8 III	F8 Iab
HR 4191 (F5 III)	$S/N = 95$	0.6	0.8	0.7
	45	0.9	1.0	1.4
	8	14	16	21
		HD 124752	HR 4301	12 Peg
		K0 V	K0 III	K0 Ib
HR 4181 (K3 III)	$S/N = 135$	0.17	0.16	0.17
	75	0.52	0.50	0.52
	30	0.63	0.52	0.61

Table 3. Errors in km/s of the radial velocities (from cross-correlation) as a function of S/N and spectral dispersion (resolution set to 2 pix).

	0.25 Å/pix		0.43 Å/pix		0.8 Å/pix		3.3 Å/pix	
	S/N	err	S/N	err	S/N	err	S/N	err
G stars	100	0.6	150	0.8	200	1.1	400	14
	70	1.0	85	2.6	120	3.6	250	35
	25	2.3	35	3.1	50	12	95	100
K stars	135	0.2	165	0.8			450	7
	75	0.5	95	1.3			260	16
	30	0.6	40	2.8			100	25

5.3.2. Detecting extra-solar planets and brown dwarfs

Gaia seems able to profitably enter the search for extra-solar planetary systems. The *Gaia* 0.1 km/s precision of the epoch radial velocities of *bright* F, G, K and M stars cannot compete with devoted ground-based searches which work in the 0.01 km/s precision regime. Ground-based searches however can hardly monitor more than a few hundred stars over some years, gathering typically 15–30 observations per target. *Gaia* may instead survey several thousands suitable targets, securing ~150 observations for each over five years. Therefore, what can make *Gaia* unique in the extra-solar planet search, is the large-number statistical approach, with a monitored sample much larger than feasible from the ground, over a longer period of time even if at $\leq 1/10$ of the ground-based precision in radial velocity.

For example, the planet recently discovered around τ Boo induces on the F7 V star a peak-to-peak amplitude of $\Delta RV = 0.93$ km/s with a period of 3.31 days. This will be an *easy* case for *Gaia*, able to provide an accurate orbital solution (if τ Boo will be not too bright for *Gaia*!). The hardest cases may be exemplified by ρ^1 55 Cnc in which a planet induces on the G8 V star an amplitude of just $\Delta RV = 0.15$ km/s with a period $P = 14.6$ days. In the latter case *Gaia* will probably be limited to spot the RV variability and to estimate the ΔRV (which constraints the planet's mass), thus providing a pruned target list for devoted follow-up ground-based programs.

The expected performances on brown dwarfs follow those estimated for extra-solar planets, the masses and orbital separations playing the difference. *Gaia* seems particularly well suited to detect brown dwarfs on wide orbits, i.e. with periods ≥ 1 yr.

5.3.3. Partnership to stellar aggregates

Fig. 5b shows the dispersion in radial velocities for 18 astrometric members of the young open cluster NGC 225, their spectral types being distributed over the interval B9 to A8. For binaries, the baricentric velocity has been used. It is evident how accurate radial velocities have detected three spurious astrometric members (at the accuracy achievable by ground-based astrometry). The observed dispersion of RV (1.7 km/s) is close to what expected from an application of the virial theorem and suggests that radial velocities

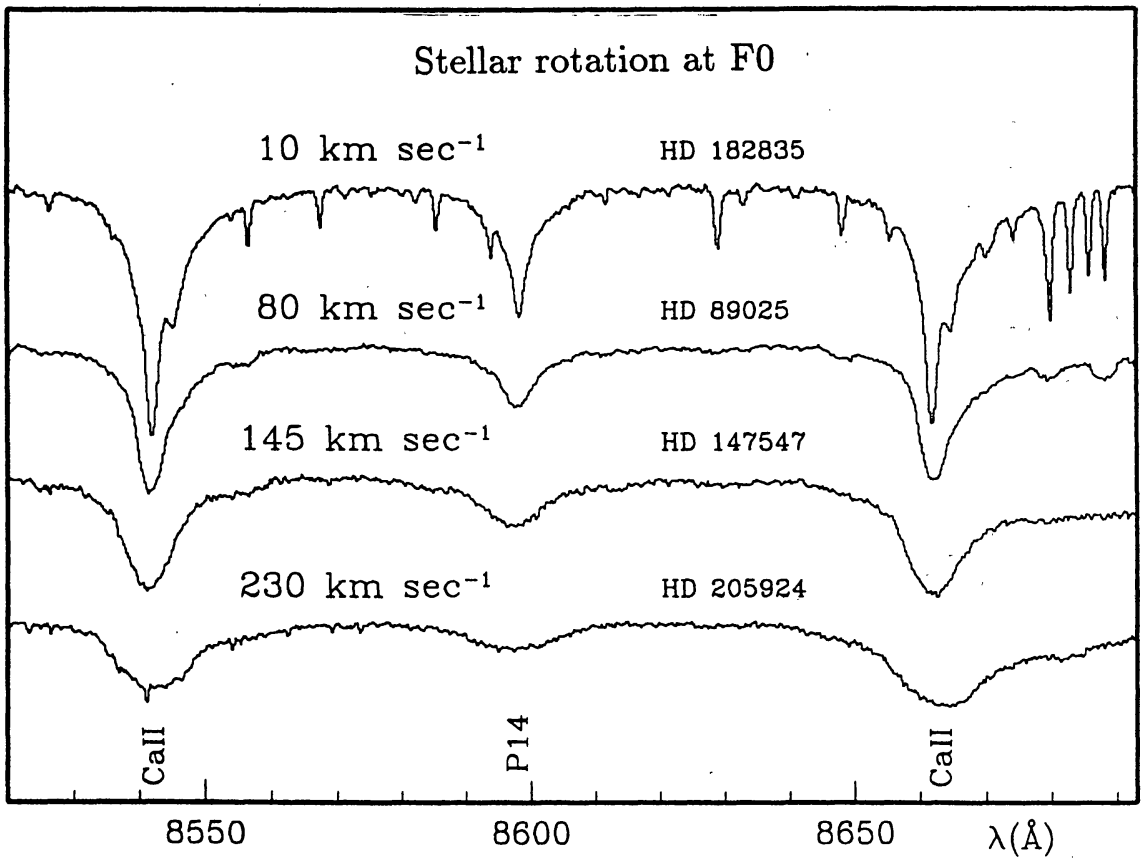

Fig. 6. Spectra of rotational velocity standards at F0. Ca II and Paschen lines offer accurate measuring tools, while weaker metallic lines are rapidly washed out after merging.

are sensitive enough to sense equipartition of the energy among the member stars.

Such accurate radial velocities (particularly the baricentric velocities of binaries) have required observations with the Asiago Echelle spectrograph extending over several years. Only those obtained in 1998 have been taken in the 8500–8750 Å range here proposed for *Gaia*. Their accuracy match quite consistently that of the older data obtained in the classical blue region. This allows us to conclude that a diagram similar to that of Fig. 5b would have been obtained if all observations had been performed in the 8500–8750 Å interval from the beginning.

5.3.4. Pulsating stars

The spectra of the three prototypes of pulsating stars, namely RR Lyr, δ Cep and o Cet (Mira) are presented in Fig. 8b. They do not present emission lines (contrary to the blue region in Miras), and therefore the pulsating activity may be accurately mapped by the variable radial velocity measured in automated cross-correlation mode. Even for the metal-poor RR Lyr (spectral class F5 with $[Z/Z_{\odot}]$=–1.4) the Ca II lines are still strong enough to provide useful RV data.

5.4. Rotational velocity

Ca II lines and to a lesser extent the Paschen lines provide a powerful tool to measure the rotational velocity. Fig. 6 shows a series of F0 spectra of increasing rotational velocity: the effect on the line profiles is outstanding. Other metallic lines are weaker than the Ca II lines and are useful only for $V_{\rm rot}\sin i \leq$30 km/s, limit over which they irremediably merge and/or wash out into the adjacent continuum. At the lowest velocities ($V_{\rm rot}\sin i \leq$30 km/s) the precision achievable on mission-spectra should be $\pm$3 km/s for F to M spectral types at the 0.25 Å/pix dispersion here used.

5.5. Mass loss

Fig. 7c presents the spectrum of P Cyg, the prototype of stars loosing mass. The effect is marked both in the Paschen and He I lines and may be detected easily even in low S/N epoch-spectra (the spectrum of Fig. 7c was intentionally underexposed to $S/N = 33$). The PSF-corrected kinetic width of the Paschen absorption components is ~34 km/s.

5.6. Peculiarities

A representative sample of peculiar and/or variable stars is shown in Figs. 7 and 8. Comments on the spectra of the pulsating variables and P Cyg have already been made.

Paschen emissions dominate the spectra of the massive X-ray binary X Per and the classical Be star ϕ Per in Figs. 7b and 7a. The emissions are so strong that they are visible on even the weakest

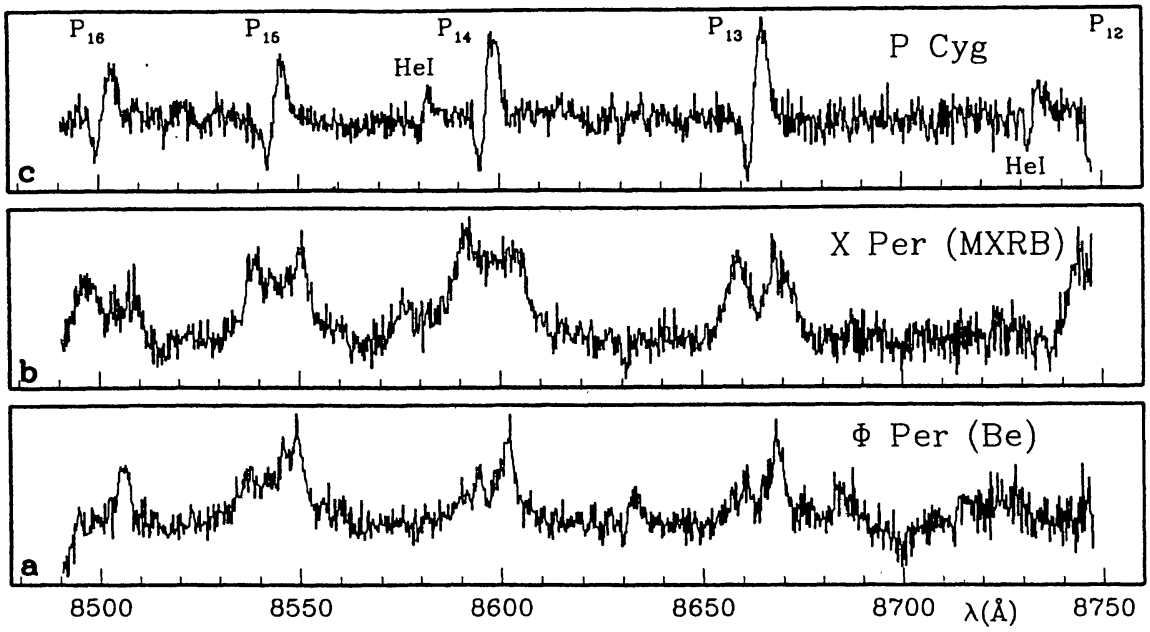

Fig. 7. Spectra of hot peculiar and variable stars. (a): spectrum of the Be star ϕ Per; (b): spectrum of the massive X-ray binary X Per; (c): signatures of wind mass-loss in the P Cyg spectrum.

epoch-spectra (the spectra in Figs. 7a,b have been intentionally underexposed, with $S/N = 26$ for X Per and $S/N = 29$ for ϕ Per).

Fig. 8a shows the spectrum of T Tau, the prototype of pre-main-sequence stars. The Ca II triplet is in strong emission, with no trace of hydrogen Paschen lines (pre-main-sequence objects are generally too cool to exhibit hydrogen lines). The Ca II lines change in shape and intensity with time, tracing the activity of the proto-star and the surrounding disk.

Fig. 8c presents spectra of three well known active stars. As for T Tau, the Paschen lines are missing while the Ca II lines have emission components (asymmetric emission cores in HR 1099 and UX Ari, a double peaked core in BY Dra). This parallels the situation in the optical range where the stars with active chromospheres generally reveal their peculiar nature not in the Balmer lines, but instead in the Ca II H and K emission.

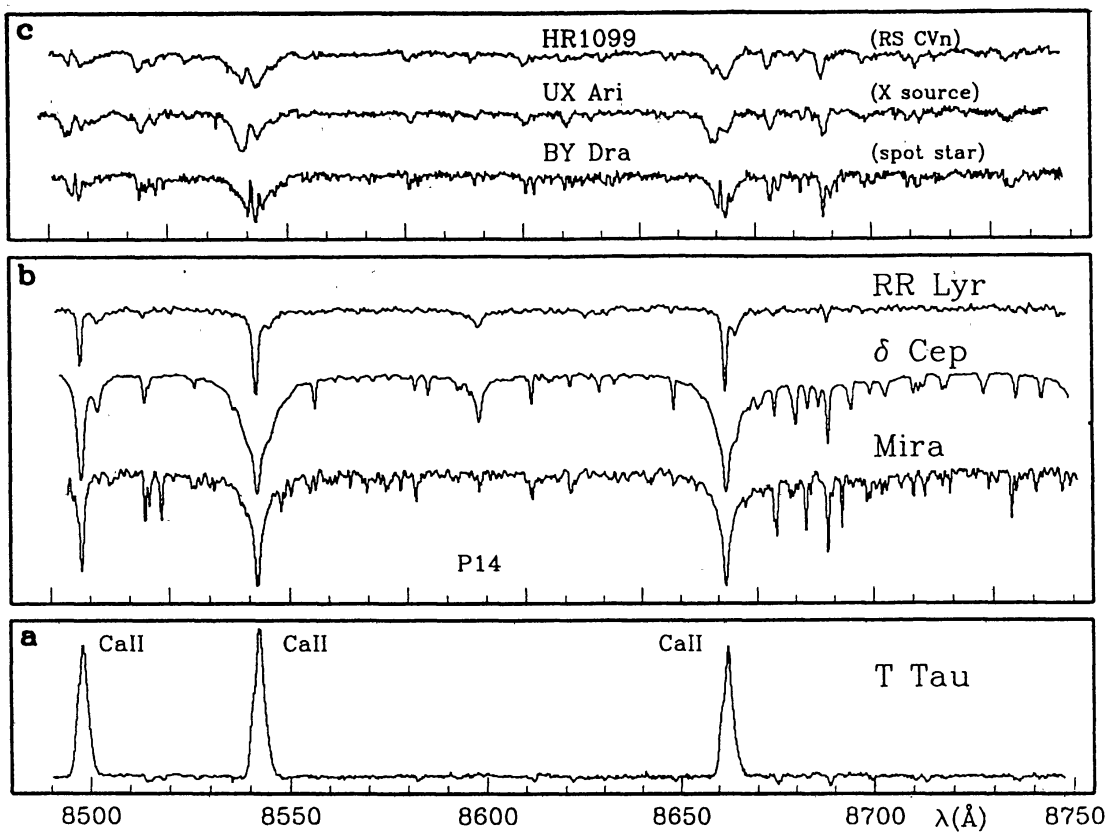

Fig. 8. Spectra of cool peculiar and variable stars. (a): very intense emission in the Ca II lines (but not in the Paschen lines) by the pre-main-sequence star T Tau; (b): zoomed-in spectra of the prototype pulsating stars; (c): zoomed-in spectra of representative active stars (emission in the cores of Ca II lines, but not in the Paschen lines).

5.7. Signatures of reddening

In the proposed 8500–8750 Å spectral interval resonant lines of metallic ions, abundant in the interstellar space, are absent. However, a medium intensity diffuse interstellar band (hereafter, DIB) at 8620 Å is present. This DIB has been so far very poorly studied in the literature. We had been therefore forced to study it from scratch, investigating if and to what extent its *EW* correlates with reddening. The results, obtained from spectra of early-type stars along the Milky Way at the galactic longitudes $80° \leq \ell \leq 210°$, are presented in Fig. 9.

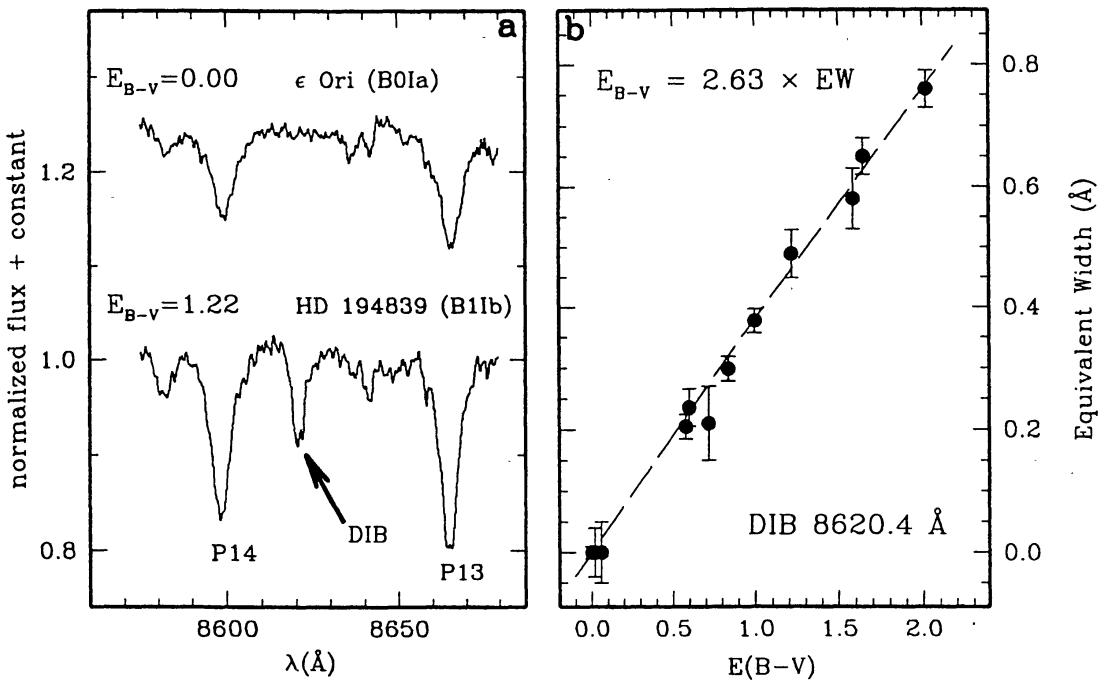

Fig. 9. The diffuse interstellar band at 8620 Å. (a): examples of unreddened and reddened stars and (b) the dependence of DIB equivalent width on reddening (the program stars in the galactic longitudes $80° \leq \ell \leq 210°$).

The correlation appears tight and the 8620 Å DIB seems to offer bright prospects as an accurate tool to estimate the reddening toward the *Gaia* spectroscopic targets.

There are DIBs in the optical range whose absorption intensity poorly correlates with E_{B-V}. In some cases there may be a real problem with the given DIB, in other cases some systematic errors, poor approach to data handling or even the use of wrong extinction law for a given direction have artificially resulted in an apparently poor correlation.

The promising results of Fig. 9 are indeed limited to a small sample of stars (randomly chosen), spread over 130° in galactic longitude. Confirmation of a tight correlation over a much larger sample of stars is desirable. Therefore, in the summer of 1998 we have started a massive observational campaign to extend as much as possible both the number of stars observed as well as the range of galactic

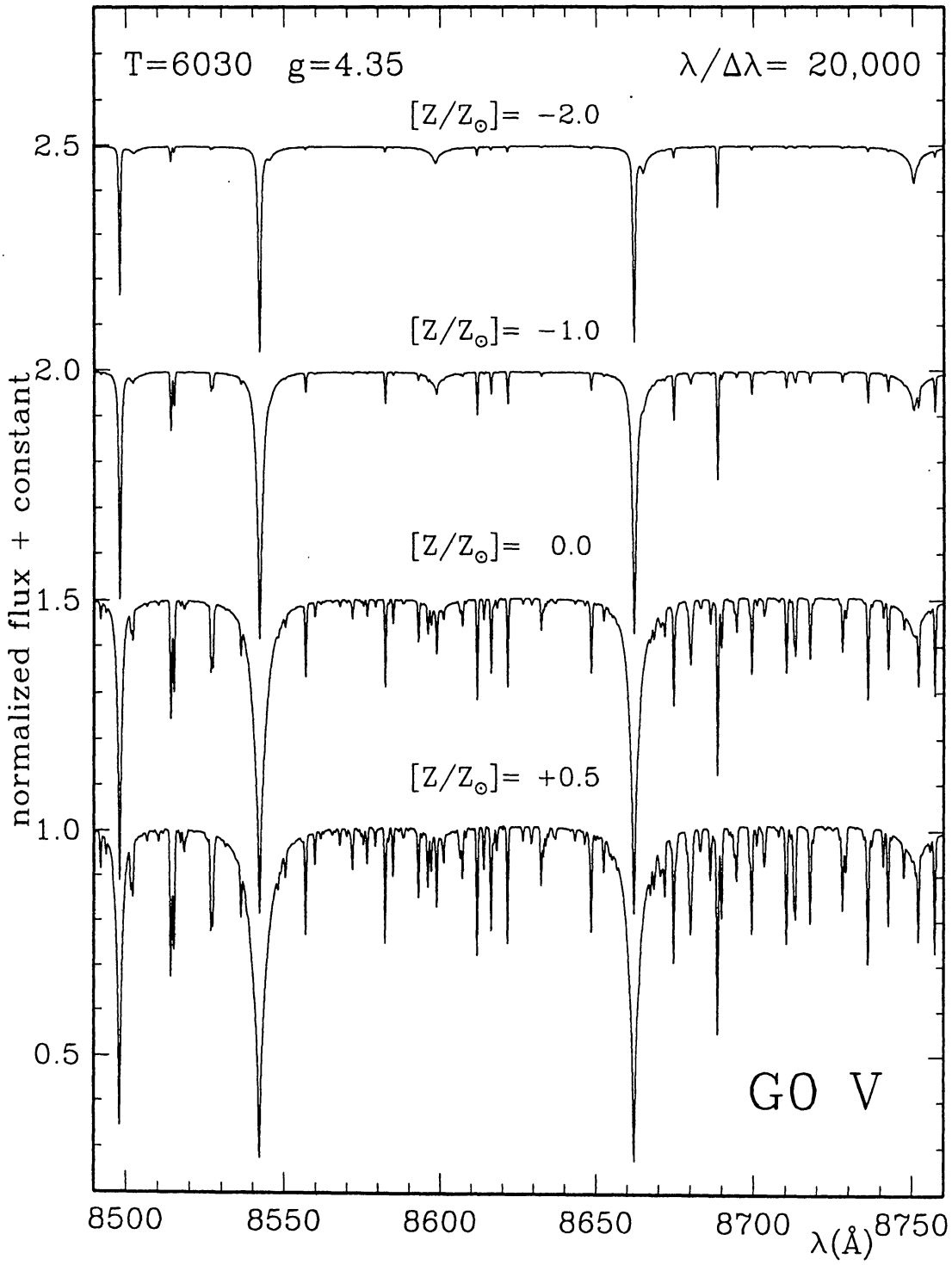

Fig. 10. Synthetic Kurucz spectra computed at the same dispersion and resolution as the observed spectra in Figs. 3 and 4 to illustrate the outstanding effects of metallicity for G0 V stars.

longitudes and distances. There might be a tight correlation in every direction, with a slope of the $EW = \mathrm{f}(E_{B-V})$ which varies with galactic longitude (reflecting changing interstellar medium). The data harvest is almost completed, data reduction is underway and a comprehensive report is expected to be submitted for publication soon.

5.8. Chemical abundances

Spectra of F, G, K and M stars show numerous and strong metallic lines over the 8500–8750 Å region, which allow an accurate chemical analysis for many elements, in particular, the iron peak and α-elements. The effect of metallicity is outstanding, as it is seen in Fig. 10 for the models of a G0 V star (note in particular Mg I 8736.000, Fe I 8514.075–8515.080 and 8688.633, Si I 8742.600 and 8556.797 Å as well as the spectacular progression of Ca II lines). Some indication on the metallicity can be even inferred in B and A stars using the strong N I lines.

6. LOWERING THE PIXEL BUDGET

A budget of 1000 pixels per spectrum could turn out to be excessive for the *Gaia* capabilities, especially in terms of telemetry to Earth and/or overlapping on the spectrometer focal plane in crowded regions. A reduction in length of the spectra can be considered, at least in principle. This can be achieved in two ways, namely:

(a) maintaining the same 8500–8750 Å range but lowering the resolution;

(b) maintaining the same resolution but shortening the wavelength interval.

The second alternative seems to minimize the loss of physical informations.

Let us consider option (a) first. A lower resolution affects the performances in all the fields considered in the above sections in a straightforward matter what can be easily guessed by considering the spectra presented in the figures. A few words are, however, due concerning the accuracy of radial velocities. Table 3 gives some preliminary results on how the accuracy of radial velocities of cool stars degrades with decreasing spectral dispersion (in all cases the spectral resolution is $\sim$2 dispersion elements). Until the dispersion

is $\leq$0.5 Å/pixel, the performance on radial velocities degrades not severely, and the epoch radial velocities still retain interest (the possibility to detect extra-solar planets will be lost, however, for dispersions $\geq$0.5 Å/pixel). Should the dispersion be $\geq$1.0 Å/pixel, the concept of the epoch radial velocities (e.g. spectroscopic orbits) will fall into serious trouble, and only the mission-averaged radial velocities will be still meaningful.

Option (b) maintains the 0.25 Å/pix dispersion but instead reduces the recorded spectrum to a minimum length (8490–8675 Å to include all three Ca II lines or 8525–8675 Å for just the two strongest Ca II lines). The accuracy of radial velocities is affected in proportion to the square root of the wavelength range (or total photon harvest for spectra dominated by absorption lines), while the derivation of rotational velocities is compromised less severely. The ability to measure the reddening will not be affected because the 8620 Å DIB lies between the two strongest Ca II lines. Spectral classification will be affected, but not hopelessly. The chemical abundance analysis seems to be most disturbed one by the reduction of the wavelength range: the majority of the metallic lines in A-type stars would be lost as the strongest lines of some important metals (e.g. Mg, Ti) in cooler stars.

ACKNOWLEDGMENTS. It is a pleasure to thank my collaborators whose help has made it possible to perform the study from scratch and on a very short time base (12 months), in particular L. Tomasella, F. Castelli, T. Tomov and L. Moro. This study has been partially supported by ASI (Italian Space Agency) contract ARS-96-175 to CISAS, University of Padova.